Exact general relativistic thin disks around black holes

José P. S. Lemos*
Departamento de Astrofísica, Observatório Nacional-CNPq, Rua General José Cristino 77, 20921 Rio de Janeiro, Brazil and Departamento di Física, Instituto Superior Tecnico, Avenida Rovisco Pais 1, 1096 Lisboa, Portugal

Patricio S. Letelier†
Departamento de Matemática Aplicada, IMECC, Universidade de Campinas, 13081 Campinas-SP, Brazil
(Received 12 April 1993; revised manuscript received 9 December 1993)

The formalism for superposing two axially symmetric exact solutions of Einstein field equations, namely, a black hole and a thin disk, is presented. Three different families of disks are analyzed. The most important family gives the first known exact solution for a black hole surrounded by a realistic heavy disk of matter. This family is the last to be analyzed. The matter of the disks is made of counterrotating particles with as many particles rotating to one side as to the other in such a way that the net angular momentum is zero and the disk is static. The first family consists of peculiar disks, in the sense that they are generated by two opposite dipoles. The particles of the disk have no pressure or centrifugal support. However, when there is a central black hole, centrifugal balance in the form of counterrotation appears. The second family is formed by disks of finite extent, the Morgan and Morgan disks. Within this family there are three parameters to play with: the black hole and disk masses, and the disk radius. These two families develop regions where matter moves with velocities greater than the velocity of light. The second family includes the remarkable configuration of a black hole surrounded by a disk made of tachyonic matter up the edge, which is at the photonic orbit. In addition some configurations have regions where the energy density is negative in violation of the weak energy condition. This is the analogue of the strut that holds two particles apart in Weyl solutions, and which has a negative energy density. The last family admits configurations which do not contain tachyonic regions and so has greater physical relevance. The disks of this family have an inner edge and a well-defined behavior at infinity. In the limit of a negligible disk mass one obtains the solution for an accretion (test-particle) disk.

PACS number(s): 04.20.Jb, 97.60.Lf

I. INTRODUCTION

After so much compelling, yet indirect, observational evidence displayed by several telescopes [1], it is now hard to doubt that giant black holes, with masses in the range $10^6 M_\odot \lesssim M_{\rm BH} \lesssim 10^{10} M_\odot$, inhabit the nuclei of active galaxies and act as the central engines that power the observed fantastic energy releases, most notably in quasars and in Seyfert galaxies. Disks, either thin or thick, are usually called on to explain the fueling mechanism into those massive and supermassive black holes, although, in contrast with binary systems of solar size masses, there is no conclusive proof for or against the presence of an accretion disk in active nuclei. However, theoretical and observational scaling arguments indicate an analogy between stellar scale phenomena, cluster of star scale phenomena, and galactic scale phenomena. Thus the black-hole–disk configuration is likely to occur and has been studied extensively.

The black-hole–disk system is difficult to treat exactly, and one must resort either to approximations or numerical schemes [2]. An approximation frequently used considers that the disk has a negligible gravitational mass in comparison with the black hole mass. This simplification can be justified only sometimes, and one should consider configurations where this is not the case [3].

Our aim here is to report some results in this direction by obtaining some pure general relativistic properties of the black-hole–thin-disk configuration, without adopting the mass-type approximations referred to above. We superpose a Schwarzschild black hole to three distinct families of thin disks: namely, (i) a peculiar dust family, (ii) the Morgan and Morgan family [4], and (iii) an annular disk family [5].

Our major simplification is that both the disk and black hole do not rotate. This non-rotation condition could be relaxed. Static disks can be interpreted in two ways. In one interpretation the matter in the disk is supported by the hoop stresses. In the other the particles move in the plane of the disk under the action of their own gravitational field in such a way that there are as many particles moving to one side as to the other. The counterrotating interpretation is frequently employed since it can be invoked to mimic true rotational effects [6]. The gravitational field of finite disks of counterrotating particles was first studied by Morgan and Morgan [4]. Infinite self-similar counterrotating disks were analyzed by Lynden-Bell and Pineault [7] and Lemos [8]. The disks of Ref. [8] include a family of topological defects which was examined by Lemos and Letelier [9]. Other static disks have also been found [10]. All these disks are infinitesimally thin [11].

Schwarzschild black holes and counterrotating thin disks are static and axisymmetric solutions of Einstein

*Electronic address: LEMOS@ON BR
†Electronic address: LETELIER@IME.UNICAMP.BR

field equations and therefore belong to the Weyl spacetimes [12]. Superposition of Weyl solutions has been extensively analyzed [13–18]. This method is very powerful, and it will allow us to discuss the gravitational properties of the astrophysically important thin disk–black-hole configuration.

In Sec. II we discuss some generic properties of disks in Weyl coordinates. In Sec. III we present Schwarzschild black holes in Weyl coordinates to set the nomenclature. In Sec. IV we develop the formalism for superposing disks and black holes. In Secs V–VII we analyze the different families of disk solutions with a black hole in the center and discuss some physical features.

II. THIN DISK SOLUTIONS IN WEYL COORDINATES

The metric for a static axially symmetric spacetime in Weyl's canonical coordinates (t,R,φ,z) is given by

$$ds^2=-e^{\phi}dt^2+e^{\nu-\phi}(dR^2+dz^2)+R^2e^{-\phi}d\varphi^2 , \tag{2.1}$$

where ϕ and ν are functions of the coordinates R and z only. Einstein field equations $R_{ab}-\frac{1}{2}g_{ab}R=8\pi T_{ab}$ ($G=c=1$) for the vacuum ($T_{ab}=0$) yield

$$\phi_{,RR}+\frac{\phi_{,R}}{R}+\phi_{,zz}=0 , \tag{2.2}$$

$$\nu[\phi]=\tfrac{1}{2}\int R\,[(\phi_{,R}{}^2-\phi_{,z}{}^2)dR+2\phi_{,R}\phi_{,z}dz] , \tag{2.3}$$

where $(\ )_{,R}\equiv\partial/\partial R$ and $(\ )_{,z}\equiv\partial/\partial z$. The integration in (2.3) is taken from the point (R,z) along the path $R(z)$ to infinity.

We now discuss a general formalism to find the energy-momentum tensor of a thin disk, given the metric potentials. Throughout this work the symbols Λ and $\nu[\Lambda]$ represent the metric potentials of the disk and ψ and $\nu[\psi]$ represent the metric potentials of the black hole. The symbols ϕ and $\nu[\phi]$ will be used generically to represent any particular Weyl solution. Black hole solutions in Weyl coordinates are C^∞, while infinitesimally thin disk solutions are C^0. The matter in such a disk behaves as a Dirac δ function in the appropriate direction. Distributions in curved spacetimes with support on three-dimensional hypersurfaces are well defined, and we use the distributional approach due to Papapetrou and Hamoui [19], Lichnerowicz [20], and Taub [21]. A different approach is given by Israel [22] where one makes use of the extrinsic curvature of thin shells. The distributional approach assumes that the metric functions are C^0.

The disk at $z=0$ divides the spacetime into two halves. The normal to the disk can be described by the covector $n_a=\partial z/\partial x^a=(0,0,0,1)$. Above the disk near $z=0$, we can expand the metric as

$$g_{ab}={g^+}_{ab}+z\left.\frac{\partial {g^+}_{ab}}{\partial z}\right|_{z=0}+\frac{1}{2}z^2\left.\frac{\partial^2 {g^+}_{ab}}{\partial z^2}\right|_{z=0}+\cdots . \tag{2.4}$$

Below the disk an analogous expansion also holds with $+\to-$. The quantity ${g^0}_{ab}$ means the value of g_{ab} at $z=0$. The discontinuities in the first derivatives of the metric can be written as (see also [21,23])

$$b_{ab}={g^+}_{ab,z}|_{z=0}-{g^-}_{ab,z}|_{z=0} . \tag{2.5}$$

Call $\Lambda^+=\Lambda(R,z)$ for $z>0$ and $\Lambda^-=\Lambda(R,-z)$ for $z<0$. Then $g^+_{tt}=-e^{\Lambda^+}$ and $g^-_{tt}=-e^{\Lambda^-}$. Using (2.5), we have

$$b_{tt}=-e^{\Lambda}(\Lambda^+{}_{,z}-\Lambda^-{}_{,z})|_{z=0}=-2e^{\Lambda}\Lambda_{,z}|_{z=0} , \tag{2.6}$$

where we have used $\Lambda^+{}_{,z}|_{z=0}=-\Lambda^-{}_{,z}|_{z=0}$ and defined $\Lambda_{,z}|_{z=0}\equiv\Lambda^+{}_{,z}|_{z=0}$. In the same way, we have

$$b_{\phi\phi}=-2R^2e^{-\Lambda}\Lambda_{,z}|_{z=0} , \tag{2.7}$$

$$b_{RR}=b_{zz}=2e^{\nu-\Lambda}(R\Lambda_{,R}-1)\Lambda_{,z}|_{z=0} . \tag{2.8}$$

From (2.6) and (2.7), one can work out (the discontinuities of) the Christoffel symbols through the disk given by

$$[\Gamma^a{}_{bc}]=\tfrac{1}{2}(\delta^z{}_b b^a{}_c+\delta^z{}_c b^a{}_b-g^{az}b_{bc}) , \tag{2.9}$$

where $[\Gamma^a{}_{bc}]\equiv\Gamma^{+a}{}_{bc}-\Gamma^{-a}{}_{bc}$ at $z=0$. From the Riemann tensor defined by

$$R_{abcd}=\tfrac{1}{2}(g_{ad,bc}-g_{bd,ac}+g_{bc,ad}-g_{ac,bd})+g_{rs}\Gamma^r{}_{ad}\Gamma^s{}_{bc}-g_{rs}\Gamma^r{}_{ac}\Gamma^s{}_{bd} ,$$

we can compute the Riemann distributional tensor given as

$$[R^a{}_{bcd}]=\tfrac{1}{2}(\delta^z{}_b\delta^z{}_c b^a{}_d-\delta^z{}_b\delta^z{}_d b^a{}_c+g^{az}\delta^z{}_c b_{bd}) . \tag{2.10}$$

Defining the Ricci distributional tensor as $[R_{ab}]=[R^c{}_{acb}]$ and the Ricci distributional scalar $[R]=[R^a{}_a]$, we can identify the distributional energy-momentum tensor $[T^a{}_b]$ on the disk through Einstein's equations as

$$[R^a{}_b]-\tfrac{1}{2}\delta^a{}_b[R]=8\pi[T^a{}_b] . \tag{2.11}$$

We can write the "true" energy-momentum tensor as $T^a{}_b=[T^a{}_b]\delta(z)$, where δ is the Dirac δ function with support on the disk. With the b_{ab} given in (2.6)–(2.8), we find through (2.9)–(2.11) the components

$$\epsilon=-T^t{}_t=e^{\Lambda-\nu}(2-R\Lambda_{,R})\Lambda_{,z}\delta(z) , \tag{2.12}$$

$$p_{\phi\phi}=T^{\phi}{}_{\phi}=e^{\Lambda-\nu}R\Lambda_{,R}\Lambda_{,z}\delta(z) , \tag{2.13}$$

$$T^R{}_R=T^z{}_z=0 . \tag{2.14}$$

Equations (2.12)–(2.14) yield the volume densities, i.e., the energy density and pressures. However, one should note that the coefficients of the δ functions in Eqs. (2.12) and (2.13) are not the true surface densities $\tau^a{}_b$. These would be given by $\tau^a{}_b=e^{(\nu-\Lambda)/2}[T^a{}_b]$.

III. BLACK HOLES IN WEYL COORDINATES

The nonrotating Schwarzschild black hole metric function ψ is given in the Weyl coordinates of Eq. (2.1) by [24]

$$\psi=\ln\frac{R_1+R_2-2m}{R_1+R_2+2m} , \tag{3.1}$$

where $R_1^2=(m-z)^2+R^2$, $R_2^2=(m+z)^2+R^2$. The other metric potential is

$$\nu=\ln\left[\frac{(R_1+R_2-2m)(R_1+R_2+2m)}{4R_1R_2}\right] . \tag{3.2}$$

For a physical interpretation of (3.1) as the potential of a Newtonian rod, see [24,25]. It is helpful to try to simplify expressions (3.1) and (3.2). In order to do that, we define the new potentials [26],

$$\mu_1=m-z+\sqrt{(m-z)^2+R^2} , \tag{3.3}$$

$$\mu_2=-m-z+\sqrt{(m+z)^2+R^2} . \tag{3.4}$$

From these we can work out other useful identities:

$$R_i=\frac{\mu_i^2+R^2}{2\mu_i} , \tag{3.5}$$

$$z_i-z=\frac{\mu_i^2-R^2}{2\mu_i} . \tag{3.6}$$

The subscript i can be 1,2. R_i is given as above, μ_i is given in (3.3) and (3.4), and $z_1=m$, $z_2=-m$. Noting that $2m=z_1-z_2$ and with the help of (3.3)–(3.6) we can now simplify (3.1) and (3.2) into

$$\psi=\ln\frac{\mu_1}{\mu_2} , \tag{3.7}$$

$$\nu=\ln\left[\frac{(R^2+\mu_1\mu_2)^2}{(\mu_1^2+R^2)(\mu_2^2+R^2)}\right] . \tag{3.8}$$

These two formulas are the ones we use when we superpose disks with black holes. Expression (3.8) can be directly found on using the property

$$\nu[\psi]=\nu[\ln\mu_2-\ln\mu_1]=\nu[\ln\mu_2]+\nu[\ln\mu_1]-2\nu[\ln\mu_1,\ln\mu_2] ,$$

with $\nu[\ln\mu_1,\ln\mu_2]=\ln(\mu_1-\mu_2)$ as shown in Ref. [14].

One can transform the metric in Weyl coordinates (t,R,φ,z) into spherical coordinates (t,r,θ,φ) by doing

$$R=\sqrt{r^2-2mr}\,\sin\theta , \quad z=(r-m)\cos\theta . \tag{3.9}$$

This coordinate transformation puts the line element (2.1) with the metric functions given in (3.7) and (3.8) into the Schwarzschild form. From (3.9) ones sees directly that the Schwarzschild radius $r=2m$ transforms into the rod $R=0$, $-m\le z\le m$. Equation (3.9) also yields that the circular equatorial photonic orbit at $r=3m$ transforms into the orbit at $R=\sqrt{3m}$. Figure 1 shows that Weyl coordinates are the natural coordinates for studying problems in which one does not need to worry about the inside of the black hole. Moreover, although a thin rod transforms into a sphere, when one passes from Weyl to Schwarzschild-type coordinates, a thin disk will not transform into a fat one when one attempts such a transformation. Under such a transformation, an infinitesimally thin disk will always remain infinitesimally thin. In addition, Weyl coordinates allow for the superposition of solutions, a subject to which we now turn.

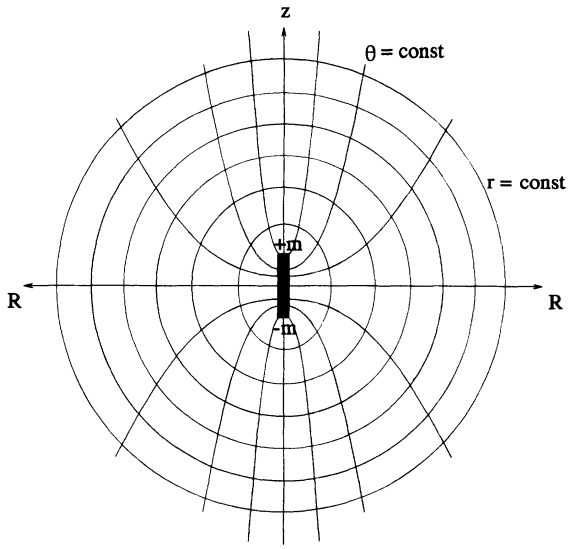

FIG. 1. Black hole is represented by the rod in Weyl coordinates (R,z). Also shown are lines of constant Schwarzschild coordinates (r,θ).

IV. FORMALISM TO SUPERPOSE THIN DISKS AND BLACK HOLES

One of the important properties of the Weyl metric (2.1) is that the field equation (2.2) for the potential ϕ is just the Laplace equation in cylindrical coordinates. Laplace's equation is linear, and thus if Λ and ψ are solutions, then the superposition $\phi=\psi+\Lambda$ is also a solution. The simplest solution of the Weyl metric is the Chazy-Curzon particle [27]. Superposing two such particles is possible [28] by introducing a strut with a negative energy density [29]. We call this the "strut problem," and we shall see that it can appear in the superposition of disks and black holes in another guise.

From (2.3) we see that the metric function $\nu[\Lambda]$ cannot be superposed since it is nonlinear. However, one can show that it obeys the relation

$$\nu[\psi+\Lambda]=\nu[\psi]+\nu[\Lambda]+2\nu[\psi,\Lambda] , \tag{4.1}$$

where

$$\nu[\psi,\Lambda]=\tfrac{1}{2}\int R[(\psi_{,R}\Lambda_{,R}-\psi_{,z}\Lambda_{,z})dR + (\psi_{,R}\Lambda_{,z}+\psi_{,z}\Lambda_{,R})dz] . \tag{4.2}$$

We now superpose ψ and Λ to obtain the energy-momentum tensor of the combined system. From (4.2) we have

$$\nu^+[\psi,\Lambda^+]_{,z}=\tfrac{1}{2}R(\psi_{,R}\Lambda^+{}_{,z}+\psi_{,z}\Lambda^+{}_{,R}) ,$$

$$\nu^-[\psi,\Lambda^-]_{,z}=\tfrac{1}{2}R(\psi_{,R}\Lambda^-{}_{,z}+\psi_{,z}\Lambda^-{}_{,R}) .$$

Thus

$$\left[\frac{\partial\nu[\psi,\Lambda]}{\partial z}\right]\equiv\left.\frac{\partial\nu^+}{\partial z}\right|_{z=0}-\left.\frac{\partial\nu^-}{\partial z}\right|_{z=0}$$
$$=\tfrac{1}{2}R\psi_{,R}(\Lambda^+{}_{,z}-\Lambda^-{}^{,z})|_{z=0}$$
$$=R\psi_{,R}\Lambda_{,z}|_{z=0} , \tag{4.3}$$

where we used

$$\Lambda^+{}_{,z}|_{z=0}=-\Lambda^-{}_{,z}|_{z=0}\equiv\Lambda_{,z}|_{z=0}\ .$$

From (2.5) we can compute the components of b_{ab}:

$$b_{tt}=-2e^{\psi+\Lambda}\Lambda_{,z}|_{z=0}\ , \tag{4.4}$$

$$b_{\phi\phi}=-2R^2e^{-\psi-\Lambda}\Lambda_{,z}|_{z=0}\ , \tag{4.5}$$

$$b_{RR}=b_{zz}=2e^{\nu-\psi-\Lambda}[R(\psi+\Lambda)_{,R}-1]\Lambda_{,z}|_{z=0}\ , \tag{4.6}$$

where $\nu=\nu[\psi+\Lambda]$. From (2.9)–(2.13) and (4.4)–(4.6), we have

$$\epsilon=-T^t{}_t=e^{\psi+\Lambda-\nu}[2-R(\psi+\Lambda)_{,R}]\Lambda_{,z}\delta(z)\ , \tag{4.7}$$

$$p_{\phi\phi}=T^\phi{}_\phi=e^{\psi+\Lambda-\nu}R(\psi+\Lambda)_{,R}\Lambda_{,z}\delta(z)\ , \tag{4.8}$$

$$T^R{}_R=T^z{}_z=0\ . \tag{4.9}$$

The nonlinearity of Einstein's equations, which shows up first in the interaction term $\nu[\psi,\Lambda]$ of (4.1), appears now in (4.7) and (4.8) in a very simple way: The potential ψ of the black hole, which corresponded to a vacuum solution, interacts with the disk and acts on the matter.

V. PECULIAR DUST DISKS AROUND BLACK HOLES

We now find a solution of a family of disks generated by gluing two spacetimes associated with two opposite dipoles. The corresponding disks are peculiar due to the presence of the negative mass coming from the dipole solution. Our aim here is to apply the methods of Sec. II to a very simple system (see also [30]). This in turn shows some interesting features associated with the superposition. To solve Laplace's equation, we start with the first spherical harmonic (with axial symmetry), $P_1(\cos\theta)=\cos\theta$. In cylindrical coordinates we have that the Weyl potential Λ is

$$\Lambda^+=\frac{\alpha^2 z}{(z^2+R^2)^{3/2}}\ ,\quad z\geq 0\ , \tag{5.1}$$

where α is a constant. For $z<0$ one interchanges z with $-z$. On using (2.3) we find

$$\nu=\frac{\alpha^4R^4}{8(z^2+R^2)^4}\left[1-8\frac{z^2}{R^2}\right]\ . \tag{5.2}$$

From (2.12) and (2.13), the energy-momentum tensor of the matter in the disk is

$$\epsilon=2\frac{\alpha^2}{R^3}e^{-\alpha^4/8R^4}\delta(z)\ , \tag{5.3}$$

$$p_{\phi\phi}=0\ . \tag{5.4}$$

The disk has an energy density profile which is zero at both extremes, $R=0$ and $R=\infty$, and has a maximum at $\alpha/(6)^{1/4}$. There is no pressure or centrifugal support. Now we superpose a black hole to this disk, using the results of Sec. IV. In analogy with the μ_1 and μ_2 potentials of the black hole of Sec. III, it is helpful to define a μ^+ potential of the disk as

$$\alpha^2\ln\mu^+=\Lambda^+\ . \tag{5.5}$$

Then, if ψ is the black hole solution as in (3.1) or (3.7), the solution of the composite system is $\phi^+=\psi+\Lambda^+=\ln[(\mu^+\mu_2)/\mu_1]$. Using (5.1), (5.5), (3.3), (3.4), and (3.7), we find

$$e^{\phi^+}=\frac{-m-z+\sqrt{(z+m)^2+R^2}}{m-z+\sqrt{(z-m)^2+R^2}}e^{\alpha^2z/(z^2+R^2)^{3/2}}\ . \tag{5.6}$$

The solution for the potential $\nu[\phi^+]$ at $z=0$ is [30]

$$\nu|_{z=0}=\frac{\alpha^4}{8R^4}+\ln\left[\frac{R^2}{R^2+m^2}\right]+\alpha^2\left[\frac{m-\sqrt{R^2+m^2}}{R(R+m-\sqrt{R^2+m^2})^2}+\frac{m+\sqrt{R^2+m^2}}{R(R-m-\sqrt{R^2+m^2})^2}\right]\ . \tag{5.7}$$

With the help of (4.7) and (4.8), we obtain the energy-momentum tensor

$$\epsilon=\frac{2\alpha^2}{R^3}e^{\phi-\nu}\left[1-\frac{m}{\sqrt{R^2+m^2}}\right]\ , \tag{5.8}$$

$$p_{\phi\phi}=\frac{2\alpha^2}{R^3}e^{\phi-\nu}\frac{m}{\sqrt{R^2+m^2}}\ , \tag{5.9}$$

where ϕ and ν are given in (5.6) and (5.7), respectively, and should be evaluated at $z=0$. Note that pressure support (or centrifugal balance) has appeared due to the presence of the black hole. Compare for this matter (5.4) and (5.9). In this sense the black hole tends to stabilize the disk, at least against ring formation.

An important quantity is the velocity V of counterrotation of the particles in the disk. One can show that it is given by [8], $V^2=p_{\phi\phi}/\epsilon$. If $p_{\phi\phi}/\epsilon>1$, then the particles in the disk travel at tachyonic or superluminal velocities. From (5.8) and (5.9), we have

$$V^2=\frac{p_{\phi\phi}}{\epsilon}=\frac{m}{\sqrt{R^2+m^2}-m}\ . \tag{5.10}$$

Thus for $R<\sqrt{3m}$ we obtain $V^2>1$. If we change to Schwarzschild coordinates as given in (3.9), we find that it corresponds to $r<3m$. This relates to the well-known result that there are no circular orbits (stable or unstable) inside the photonic orbit. Since we are superposing systems, the combined solution is giving the consistent result that the centrifugal-gravity balance inside the Schwarzschild radius $r=3m$ can only be maintained for superluminal velocities. From Eq. (5.8) we find $\epsilon\geq 0$ always. However, the analogue to the "strut problem" mentioned in Sec. IV is the existence of tachyonic matter. Although the existence of tachyonic matter has not been dismissed [31], we do not press this matter further.

One can generate a family of disks from this first member found through the first spherical harmonic P_1. One has simply to consider all the other harmonics with axial symmetry, $P_2, P_3, \ldots, P_n$, etc.

VI. MORGAN-MORGAN DISKS AROUND BLACK HOLES

The Morgan-Morgan disks [4] have an outer edge. We now have three parameters to play with: the mass m of the black hole and the mass M and radius R of the disk. This family has an infinite countable number of members [14]. Here we superpose the first member of the family with a black hole (the zeroth member has a singular surface energy density at the edge); see also [32]. The source of the gravitational field of the disk has the associated Newtonian density

$$S=\frac{3M}{2\pi a^2}(a^2-R^2)^{1/2}\delta(z) , \tag{6.1}$$

which corresponds to the monopole plus quadropole term. The metric potentials were originally given in oblate ellipsoidal coordinates (ζ,η) connected to the Weyl cylindrical coordinates by

$$R^2=a^2(1+\zeta^2)(1-\eta^2) , \tag{6.2}$$

$$z=a\zeta\eta , \tag{6.3}$$

with $-1\le\eta\le 1$ and $0\le\zeta<\infty$. The t and φ coordinates are the same in both systems. The disk itself has oblate coordinates given by $\zeta=0$ and $-1\le\eta\le 1$ and Weyl coordinates given by $z=0$ and $R\le a$. In oblate elliptical coordinates, the metric potentials Λ and $\nu[\Lambda]$ are

$$\Lambda=-\frac{2M}{a}\{\operatorname{arccot}\zeta+\tfrac{1}{4}[(3\zeta^2+1)\operatorname{arccot}\zeta-3\zeta]\times(3\eta^2-1)\} , \tag{6.4}$$

$$\nu=\frac{9}{2}\frac{M^2}{a^2}\frac{R^2}{a^2}\left[\frac{R^2}{a^2}B^2(\zeta)-(1+\eta^2)A^2(\zeta)-2\zeta(1-\eta^2)A(\zeta)B(\zeta)\right] , \tag{6.5}$$

where R is given in (6.2) $A=\zeta\operatorname{arccot}\zeta-1$, and $B=\frac{1}{2}[\zeta/(1+\zeta)-\operatorname{arccot}\zeta]$. Note that Λ and ν are continuous everywhere and vanish at infinity. However, at the disk their derivatives are singular due to the δ function in (6.1). One can also use the μ formalism of Refs. [13,14] by writing

$$\mu=ia-z+s , \tag{6.6}$$

$$s=[(ia-z)^2+R^2]^{1/2} \tag{6.7}$$

and

$$a\zeta=\mathrm{Re}s , \tag{6.8}$$

$$a\eta=-\mathrm{Im}s . \tag{6.9}$$

Then (6.4) with the help of (6.6)–(6.9) transforms into

$$\Lambda=-\frac{3M}{a^3}\mathrm{Im}\left[\left(a^2+z^2-\frac{R^2}{2}\right)\ln\mu+\frac{1}{2}(3z+ia)s\right] \tag{6.10}$$

and similarly for the potential ν, although it is a much longer expression, which it is not necessary to write down. Fortunately, we are interested in the plane $z=0$ where these formulas simplify considerably. On the disk, Eqs. (6.4) and (6.5) reduce to

$$\Lambda=-\frac{3\pi}{2}\frac{M}{a}\left[1-\frac{1}{2}\frac{R^2}{a^2}\right] , \tag{6.11}$$

$$\nu=\frac{9}{2}\frac{M^2}{a^2}\frac{R^2}{a^2}\left[\left[1+\frac{\pi^2}{16}\right]\frac{R^2}{a^2}-2\right] . \tag{6.12}$$

Using now Eqs. (2.12) and (2.13) or otherwise, we can compute the nonzero components of the energy-momentum tensor:

$$\epsilon=F\left[1-\frac{R^2}{a^2}\right]^{1/2}\left[1-\frac{3\pi}{4}\frac{MR^2}{a^3}\right]\delta(z) , \tag{6.13}$$

$$p_{\phi\phi}=F\left[1-\frac{R^2}{a^2}\right]^{1/2}\frac{3\pi}{4}\frac{MR^2}{a^3}\delta(z) , \tag{6.14}$$

where $F=(3M/2\pi a)e^{\Lambda-\nu}$, with Λ and ν given in (6.11) and (6.12), respectively. One of the requirements of the weak energy condition is $\epsilon>0$ everywhere. It is easier to violate this condition at the edge. Using (6.13), this gives $M/a<4/3\pi$. The counterrotating velocity is

$$V^2\equiv\frac{p_{\phi\phi}}{\epsilon}=\frac{(3\pi/4)MR^2/a^2}{1-(3\pi/r)MR^2/a^2} . \tag{6.15}$$

The largest velocity occurs at the edge $R=a$. Thus, if the particles are to move with speeds less than the speed of light, then $M/a<2/3\pi$. This is a stronger limit than the one given by the $\epsilon>0$ condition above. For $M/a>2/3\pi$, there are particles moving at tachyonic or superluminal velocities $V>1$.

Up to now we have made a summary of the work of Morgan and Morgan. If we now superpose a black hole of mass m at the center of the disk, then using (3.9), (6.4), (4.9) and (4.10) we find the surface energy density and pressure:

$$\epsilon=G\left[1-\frac{R^2}{a^2}\right]^{1/2}\left[1-\left[\frac{3\pi}{4}\frac{MR^2}{a^3}+\frac{m}{\sqrt{m^2+R^2}}\right]\right]\delta(z) , \tag{6.16}$$

$$p_{\phi\phi}=G\left[1-\frac{R^2}{a^2}\right]^{1/2}\left[\frac{3\pi}{4}\frac{MR^2}{a^3}+\frac{m}{\sqrt{m^2+R^2}}\right]\delta(z) , \tag{6.17}$$

where G is a known, although long, expression, involving the superposed Weyl potentials. The condition $\epsilon\ge 0$ is equivalent to

$$f(x)\ge 0, \quad 0\le x\le x_{\text{edge}} , \tag{6.18}$$

where

$$f(x)=\sqrt{x^2+1}(1-2\lambda\sigma^2x^2)-1 , \tag{6.19}$$

with $x\equiv R/m$, $\lambda\equiv(3\pi/8)M/a$, and $\sigma=m/a$. Equation (6.19) has two zeros, the inner x_i and the outer x_o given by

$$x_i=0 \tag{6.20}$$

and

$$x_0^2=\frac{1-\lambda\sigma^2-\sqrt{\lambda\sigma^2(\lambda\sigma^2+2)}}{2\lambda\sigma^2} . \tag{6.21}$$

In between these two zeros, the energy density is positive. In order to have $x_o^2\geq 0$, Eq. (6.21) implies

$$4\lambda\sigma^2\leq 1 , \text{ i.e., } \frac{Mm^2}{a^3}\leq\frac{2}{3\pi} . \tag{6.22}$$

This tells us that there is a maximum product between the disk mass and the black hole mass, given by $Mm^2/a^3=2/3\pi$. The edge of the disk is at $x_{\text{edge}}=a/m$. To have $\epsilon\geq 0$ everywhere, we impose $x_{\text{edge}}\leq x_o$, i.e.,

$$\frac{1}{\sigma^2}\leq\frac{1-\lambda\sigma^2-\sqrt{\lambda\sigma^2(\lambda\sigma^2+2)}}{2\lambda\sigma^2} .$$

One can simplify this further to give

$$\sqrt{\lambda\sigma^2(\lambda\sigma^2+2)}\leq 1-\lambda(2+\sigma^2) . \tag{6.23}$$

Equation (6.23) is valid only if

$$0\leq\sigma^2\leq\frac{(1-2\lambda)^2}{4\lambda(1-\lambda)^2} \tag{6.24}$$

and

$$\sigma^2\leq\frac{1}{\lambda}-2 . \tag{6.25}$$

From (6.25) one has $0\leq\lambda\leq\frac{1}{2}$, i.e., $M/a\leq 4/3\pi$, which is just the Morgan-Morgan condition. Within these constraints for M the condition that actually holds for m is (6.24), which can be written as

$$0\leq\left[\frac{m}{a}\right]^2\leq\frac{[1-(3\pi/4)M/a]^2}{(3\pi/2)(M/a)[1-(3\pi/8)M/a]^2} . \tag{6.26}$$

When $M/a\to 0$ the right-hand equality in Eq. (6.26) holds for $(m/a)\simeq\sqrt{2/3\pi M/a}$. If the black hole mass is greater than this value, there must be a region of antigravity where $\epsilon<0$, in violation to the weak energy condition. On the other hand, for $M/a=(4/3\pi)(1-2\delta)$ with $\delta\ll 1$, the right-hand equality holds for $m/a\simeq\delta$. Thus highly diluted disks ($M/a\to 0$) permit that relatively massive black holes sit in their centers, while highly compact disks ($M/a\to 4/3\pi$) allow only for the existence of light black holes, with masses negligible with respect to the disk mass. These are the limits imposed by the $\epsilon\geq 0$ condition. However, we know the more tight condition, sometimes called the dominant energy condition, which states that the particles should move with speeds less than the speed of light.

From (6.16) and (6.17), we find

$$V^2\equiv\frac{p_{\phi\phi}}{\epsilon}=\frac{(3\pi/4)MR^2/a^3+m/(\sqrt{m^2+R^2})}{1-[(3\pi/4)MR^2/a^3+m/(\sqrt{m^2+R^2})]} . \tag{6.27}$$

The condition $V^2\leq 1$ is equivalent to

$$g(x)\geq 0 , \tag{6.28}$$

with

$$g(x)=\sqrt{x^2+1}(1-4\lambda\sigma^2x^2)-2 . \tag{6.29}$$

From Eq. (6.29) one finds that there are two characteristic radii: the inner and the outer light radii. Matter between the event horizon $R/a=0$ and the inner light radius has tachyonic speeds. This is a necessary evil of this type of solution. It means that if one put matter near the black hole (as we are obliged to do in this superposition of exact solutions), the matter orbits at exceedingly high speeds in that region. Note also that the inner light radius is a discontinuous function of the black hole mass at $m=0$. When the black hole has zero mass $m=0$, there is no inner light radius. However, for any other mass, no matter how small, an inner light radius appears.

Farther out from the inner light radius, the velocity of the particles decreases up to a certain radius. Then the gravitational field of the disk takes over that of the black hole, and the particles start to speed up, until they again move at light velocities. This is the outer light radius. One can impose that the outer edge of the disk is at the other light radius, which in turn gives a condition on m and M. Indeed, using (6.29), one finds that $V^2<1$ at $R=a$ gives

$$0\leq\left[\frac{m}{a}\right]^2\leq\frac{1-(3\pi/2)M/a}{3[1+(\pi/2)M/a]} . \tag{6.30}$$

When there is no black hole, $m=0$, one has from (6.30) $M/a\leq 2/3\pi$, which is just the Morgan-Morgan condition. From (6.30) one can work out that there is a maximum value for the product Mm^2. It is given by $Mm^2/a^3\lesssim 0.042(2/3\pi)$. [Note that this is much tighter than the maximum value given by Eq. (6.22) derived from the $\epsilon\geq 0$ condition.] When the equality holds, i.e., $Mm^2/a^3=0.042(2/3\pi)$, the inner and outer light radii coincide. In such a case, one has the remarkable configuration of a black hole surrounded by a disk made of pure tachyonic matter. In this case the black hole mass is $m/a\simeq 1/2.63$ and the ratio of the black hole

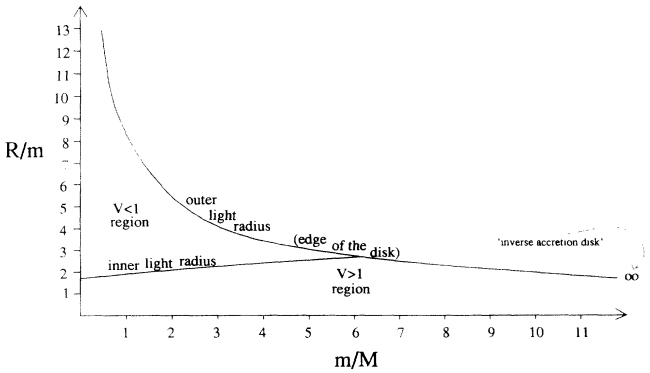

FIG. 2. Outer edge and inner light radius of the Morgan-Morgan disks plus black hole extreme configurations are shown. Each system is specified by the ratio m/M. (By extreme it is meant $V=1$ at the other edge.)

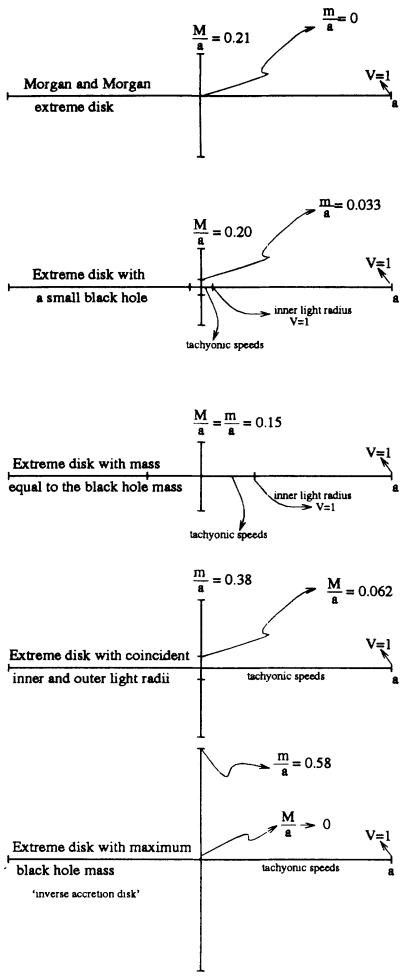

FIG. 3. Representative configurations of extreme cases within the Morgan-Morgan plus black hole family. Weyl coordinates (R,z) are being used.

mass to the disk mass is $m/M \simeq 6.2$. When $M/a \to 0$, then $m/a \to 1/\sqrt{3}$; i.e., there is a disk made of test particles (negligible mass) with tachyonic speeds up to the outer edge where $V=1$. This is the even more remarkable configuration of a disk of tachyonic matter situated in between the event horizon and the photonic orbit at $R=\sqrt{3}m$. We can call it the "inverse accretion disk." In Fig. 2 we plot the inner and outer light radii as a function of the ratio m/M. In Fig. 3 we draw various representative configurations for the case in which inequality in (6.30) is saturated. When the inequality in (6.30) is not saturated, i.e., when the velocity of the matter at the edge is less than the velocity of the light, there are other possible interesting configurations. For lower velocities at the edge, one can have ratios $M/m \ll 1$.

VII. ANNULAR DISKS AROUND BLACK HOLES

The previous three families, although displaying surprising results, showed unwanted features such as tachyonic and negative density regions. In order to overcome this problem, we now comment on a family of disks which does not have these problems. In the superposition of these disks with a black hole, tachyonic regions develop because there is matter up to the event horizon. Therefore, to suppress those regions, one has to have a disk solution with an inner edge. Then one may impose the less than the speed of light condition throughout the disk.

The simplest way to achieve this is to make an inversion (i.e., a Kelvin transformation [33]) on the Morgan-Morgan family. Here we discuss the superposition of the first member of the family with a black hole. Let $\Lambda(R,z)$ be a solution of the Poisson equation (2.2), with the associated Newtonian density [see Eq. (6.4)] $\rho=S(R)\delta(z)$. Then, under inversion, $R^2+z^2 \to a^4/(R^2+z^2)$ (where a is some constant), one can show that

$$\bar{\Lambda}(R,z)=\frac{a}{\sqrt{R^2+z^2}}\Lambda\left[\frac{a^2R}{R^2+z^2},\frac{a^2z}{R^2+z^2}\right]$$

is also a solution with an associated Newtonian density

$$\bar{S}(R)=\left[\frac{a}{R}\right]^3 S\left[\frac{a^2}{R}\right]\delta(z)\ .$$

The inversion of the first member of the Morgan-Morgan family gives the potential Λ^A of the annular disk:

$$\Lambda^A=-\frac{4\bar{M}a^2}{\pi r^5}\mathrm{Im}\left[\left[z^2-\frac{1}{2}R^2+\frac{r^4}{a^2}\right]\ln\bar{\mu}+\frac{1}{2}\left[3z+i\frac{r^2}{a}\right]\bar{s}\right], \tag{7.1}$$

where $r=(R^2+z^2)^{1/2}$

$$\bar{s}=\left[\left[-z+i\frac{r^2}{a}\right]^2+R^2\right]^{1/2},$$

$\bar{\mu}=-z+ir^2/a+\bar{s}$, and $\bar{M}$ is the mass of the annular disk. Asymptotically, $r\to\infty$, and one has $\Lambda_A=-2\bar{M}/r$, as expected for a Chazy-Curzon particle. It is not trivial to find the other Weyl potential ν_A by analytical methods, and we do not attempt it here. However, the regularity condition on the axis, $\nu\to 0$ as $R\to 0$, can always be satisfied by choosing appropriately the constant of integration for ν_A. Now if we use Eqs. (4.7)–(4.9), we find, for the combined black hole plus annular disk system, the following expressions valid for $R\geq a$:

$$\epsilon=\bar{G}\left[1-\frac{a^2}{R^2}\right]^{1/2}\left\{1-\left[\frac{\bar{M}}{R}\left[1-\frac{3}{2}\frac{a^2}{R^2}\right]+\frac{m}{\sqrt{R^2+m^2}}\right]\right\}, \tag{7.2}$$

$$p_{\phi\phi}=\bar{G}\left[1-\frac{a^2}{R^2}\right]^{1/2}\left[\frac{\bar{M}}{R}\left[1-\frac{3}{2}\frac{a^2}{R^2}\right]+\frac{m}{\sqrt{R^2+m^2}}\right], \tag{7.3}$$

where, as before, $\bar{G}$ is an expression involving the superposed Weyl potentials. At $R=a$ one has $\epsilon(a)=p_{\phi\phi}(a)=0$. For $R\to\infty$ the fields behave as

$\epsilon = O(1/R^3)$, $p_{\phi\phi} = O(1/R^4)$. The condition $\epsilon \geq 0$ is always satisfied for any values of $\bar{M}/a$ and m/a. One can also look for the sign of $p_{\phi\phi}$ throughout the disk, although we should note that there is no obstacle of having any sign. The condition that $p_{\phi\phi} \geq 0$ is $\bar{M}/a \leq 2m/a/[\sqrt{1+(m/a)^2}]$. For $m/a = 0$ there is no configuration with positive pressure everywhere, since in the region $a < R < (\frac{3}{2})^{1/2}a$ the disk is composed of matter with tension. On the other hand, for any nonzero value of m/a there are always configurations which have no tension regions. As before, the condition that the particles move with speeds less than the speed of light is

$$V^2 \equiv \frac{p_{\phi\phi}}{\epsilon} = \frac{\frac{\bar{M}/a}{R/a}\left[1-\frac{3}{2}\frac{1}{(R/a)^2}\right]+\frac{m/a}{\sqrt{(R/a)^2+(m/a)^2}}}{1-\left[\frac{\bar{M}/a}{R/a}\left[1-\frac{3}{2}\frac{1}{(R/a)^2}\right]+\frac{m/a}{\sqrt{(R/a)^2+(m/a)^2}}\right]} \leq 1 . \quad (7.4)$$

A careful study of Eq. (7.4) shows that there are some interesting configurations free of tachyonic matter. For the no-black-hole configuration $m/a = 0$, the maximum velocity of the matter is attained at $R = (\frac{9}{2})^{1/2}a \simeq 2.1a$. In this case the equality in (7.4) holds when $\bar{M}/a \simeq 1.6$. Thus, from the inner edge $R = a$ up to $R = (\frac{3}{2})^{1/2}a$, the disk is composed of matter with tension. At $R = (\frac{3}{2})^{1/2}a$, the disk is made of dust matter; i.e., the particles do not rotate. From then onwards they start to counterrotate and achieve their maximum velocity at $R = (\frac{9}{2})^{1/2}a$, which for $\bar{M}/a \simeq 1.6$ is equal to the speed of light. For $R \to \infty$ one has that the velocity of the matter is $V^2 \sim \bar{M}/R$.

A necessary condition to have tachyonic free disks is $0 \leq m/R_{\max} \leq 1/\sqrt{3}$, where $R_{\max}$ is the radius in which the matter has the highest velocity. An interesting possible configuration is $m/a = 1/\sqrt{2}$. The matter achieves maximum speed at $R/a = (\frac{3}{2})^{1/2}$ which is equal to the velocity of the light when $\bar{M}/a \simeq 0.7$. There is no tension region in this disk, and for $R \to \infty$ one has that the velocity of the matter is $V^2 \sim (\bar{M}+m)/R$. Another disk which is worth comment is the test particle disk $\bar{M}/a \to 0$. The maximum velocity is at the inner edge $R = a$. This particular configuration corresponds to the non-self gravitating accretion disk surrounding a Schwarzschild black hole. For $m/a = 1/\sqrt{3}$, the maximum velocity is the velocity of light. This is precisely the test particle disk which extends up to the photonic orbit at $R = \sqrt{3m}$. At $R \to \infty$ the matter rotates with speed $V^2 \sim m/R$, as expected. If one wishes, one can choose the parameters in such a way that the inner edge lies at the last stable orbit, thus mimicking a true accretion disk [34].

VIII. CONCLUSIONS

In this work we have described a method which can be used to superpose counterrotating thin disks and black holes. We have also analyzed three families. The first two families show in a clear way the existence of the inner photonic orbit and the appearance of matter with superluminal velocities in between this orbit and the black hole. The second family yields solutions which can be considered interesting since one can extract some pure gravitational information from the systems. However, these solutions give (inside the inner photonic orbit) matter moving at superluminal velocities, which cannot be considered realistic. In order to eliminate this problem, we have considered the superposition of an annular disk with a black hole. This family, having an inner edge, allowed us to present plausible configurations free of nonphysical regions. An effect that can also be analyzed is the distortion of the event horizon due to the presence of the disk [35]. Other effects needed to be discussed are geodesic trajectories, the redshift of photons emitted within the system, thermodynamics, and Hawking radiation.

ACKNOWLEDGMENTS

One of us (J.P.S.L.) thanks the Departamento de Matemática Aplicada da Universidade de Campinas for the hospitality while this work was being initiated, a grant from CNPq-Brazil, and a grant from JNICT-Portugal to finish this work at Instituto Superior Técnico de Lisboa.

[1] See J. Kormendy and D. Richstone, Astrophys. J. **393**, 559 (1992), for evidence that gaint black holes exist in active galactic nuclei. See also D. Lynden-Bell, Nature (London) **223**, 690 (1969).

[2] M. C. Begelman, R. D. Blandford, and M. J. Rees, Rev. Mod. Phys. **56**, 255 (1984). For numerical calculations, see A. Lanza, Astrophys. J. **389**, 141 (1992); S. Nishida, Y. Eriguchi, and A. Lanza, in *13th Conference of General Relativity and Gravitation, Abstracts of Contributed Papers*, edited by P. W. Lamberti and O. E. Ortiz (Universidad Nacional de Córdoba, Córdoba, Argentina, 1992).

[3] P. Wiita, Phys. Rep. **123**, 118 (1985); J. Goodman, and R. Narayan, Mon. Not. R. Astron. Soc. **231**, 17 (1988); S. K. Chakrabarti, J. Astrophys. Astron. **9**, 49 (1988).

[4] T. Morgan and L. Morgan, Phys. Rev. **183**, 1097 (1969).

[5] J. P. S. Lemos and P. S. Letelier (unpublished).

[6] See for spherical systems, A. Einstein, Ann. Math. **40**, 924 (1939); and for cylindrical systems, see T. A. Apostolatos and K. S. Thorne, Phys. Rev. D **46**, 2435 (1992).

[7] D. Lynden-Bell and S. Pineault, Mon. Not. R. Astron. Soc. **185**, 679 (978).

[8] J. P. S. Lemos, Class. Quantum Grav. **6**, 1219 (1989); Mon. Not. R. Astron. Soc. **230**, 451 (1988); J. P. S. Lemos and O. S. Ventura, "Planar and Axisymmetric Walls in General

Relativity: a Comparison," Observatório Nacional report, 1993 (unpublished) [J. Math. Phys. (to be published)].

[9] J. P. S. Lemos and P. S. Letelier, Phys. Lett. A **153**, 288 (1991).

[10] J. Bicák, D. Lynden-Bell, and J. Katz, Phys. Rev. D **47**, 4334 (1993); J. BicáK, D. Lynden-Bell, and C. Pichon, Mon. Not. R. Astron. Soc. (to be published); D. Lynden-Bell and C. Pichon (unpublished).

[11] We mention that rotating thin disks have been analyzed in various papers. Numerical work: J. M. Bardeen and R. V. Wagoner, Astrophys. J. **167**, 359 (1971); J. M. Bardeen, in *Black Holes,* edited by C. DeWitt and B. DeWitt (Gordon and Breach, New York, 1973); E. M. Butterworth and J. R. Ipser, Astrophys. J. **204**, 200 (1976); E. M. Butterworth, *ibid.* **204**, 561 (1976); T. Nakamura, K. Oohara, and Y. Kojima, Prog. Theor. Phys. Suppl. **90**, 1 (1987); see also Lanza in Ref. [2]. Approximation schemes: D. Lynden-Bell and S. Pineault, Mon. Not. R. Astron. Soc. **185**, 695 (1978); P. S. Wesson, Astrophys. Space Sci. **57**, 203 (1978); see also [8]. Exact solutions; J. Bicák and T. Ledvinka, Phys. Rev. Lett. **71**, 1699 (1993); D. Lynden-Bell and C. Pichon, report at the Dedication Symposium, IUCAA, Pune, India, 1993 (unpublished).

[12] D. M. Zypoy, J. Math. Phys. **7**, 1137 (1966); B. H. Voorhees, Phys. Rev. D **2**, 2119 (1970); D. Kramer, H. Stephani, M. MacCallum, and E. Herlt, *Exact Solutions of Einsteins's Field Equations* (Cambridge University Press, Cambridge, England, 1980).

[13] P. S. Letelier, J. Math. Phys. **26**, 467 (1985).

[14] P. S. Letelier and S. R. Oliveira, J. Math. Phys. **28**, 165 (1987).

[15] P. S. Letelier and S. R. Oliveira, Class. Quantum Grav. **5**, L47 (1988). See also references therein.

[16] For superposition of topological defects solutions, see P. S. Letelier, Class. Quantum Grav. **4**, L75 (1987); **6**, L207 (1989); **7**, L203 (1990); Phys. Rev. Lett. **66**, 268 (1991); Class. Quantum Grav. **8**, L137 (1991); **9**, 2057 (1992).

[17] J. P. S. Lemos and P. S. Letelier, Gen. Relativ. Gravit. **25**, 365 (1993).

[18] The superposition of a rotating black hole with a thin bubble has been recently considered by P. S. Letelier and A. Wang (unpublished).

[19] A. Papapetrou and A. Hamoui, Ann. Inst. Henri Poincaré **9**, 179 (1968).

[20] A. Lichnerowicz, C.R. Acad. Sci. **273**, 528 (1971).

[21] A. H. Taub, J. Math. Phys. **21**, 1423 (1980).

[22] W. Israel, Nuovo Cimento B **44**, 1 (1966).

[23] P. S. Letelier and A. Wang, "Topological Defects: a Distribution Theory Approach," Report No. IMECC-DMA preprint, Universidade de Campinas, 1993 (unpublished).

[24] H. P. Robertson and T. W. Noonan, *Relativity and Cosmology* (Saunders, Philadelphia, 1969), p. 272; Kramer *et al.* in Ref. [12].

[25] W. B. Bonnor, Gen. Relativ. Gravit. **15**, 535 (1983).

[26] These potentials appear naturally in the inverse scattering formalism of V. A. Belinski and V. E. Zakharov, Zh. Eksp. Teor. Fiz. **75**, 1955 (1978) [Sov. Phys. JETP **48**, 985 (1978)]. See also Refs. [13] and [14].

[27] M. J. Chazy, Bull. Soc. Math. France **52**, 17 (1924), H. E. J. Curzon, Proc. London Math. Soc. **23**, 477 (1924).

[28] A. Einstein and N. Rosen, Phys. Rev. **49**, 404 (1936).

[29] The strut is in effect a topological defect where the effective gravitational mass density is zero, although its energy density is negative. See [15] and [16].

[30] J. P. S. Lemos and P. S. Letelier, "Two New Families of Exact Disks with a Central Black Hole," report, 1993 (unpublished).

[31] J. V. Narlikar and E. C. G. Sudarshan, Mon. Not. R. Astron. Soc. **175**, 105 (1976); E. C. G. Sudarshan, *Symposia on Theoretical Physics and Mathematics* (Plenum, New York, 1970), Vol. 10, p. 129.

[32] J. P. S. Lemos and P. S. Letelier, Class. Quantum Grav. **10**, L75 (1993).

[33] W. Thomson, J. Math. Pure Appl. **12**, 256 (1847); O. D. Kellog, *Foundations of Potential Theory* (Dover, New York, 1953).

[34] M. Anderson and J. P. S. Lemos, Mon. Not. R. Astron. Soc. **233**, 489 (1988).

[35] R. Geroch and J. B. Hartle, J. Math. Phys. **23**, 680 (1982).